

TOPOLOGICAL RECURSION FOR SYMPLECTIC VOLUMES OF MODULI SPACES OF CURVES

JULIA BENNETT, DAVID COCHRAN, BRAD SAFNUK, AND KAITLIN WOSKOFF

ABSTRACT. We construct locally defined symplectic torus actions on ribbon graph complexes. Symplectic reduction techniques allow for a recursive formula for the symplectic volumes of these spaces. Taking the Laplace transform results in the Eynard-Orantin recursion formulas for the Airy curve $x = \frac{1}{2}y^2$.

CONTENTS

1. Introduction	1
2. Background	4
3. Local Structure	12
4. Recursion formula	16
5. Virasoro constraints	19
6. Eynard-Orantin recursion	21
References	24

1. INTRODUCTION

Since Kontsevich's proof [21] of the Witten conjecture [37], there has been a flurry of activity centered around the tautological ring of the moduli space of curves, and expanded more generally to Gromov-Witten invariants. However, many of the fundamental tools developed by Kontsevich have remained comparatively ignored.

In this paper we focus on the combinatorially defined 2-form $\Omega_{\vec{L}}$ used by Kontsevich to represent the scaled sum of ψ -classes

$$[\Omega_{\vec{L}}] = \frac{1}{2}(L_1^2\psi_1 + \cdots L_n^2\psi_n).$$

In particular, this form leads to a family of symplectic structures on the moduli space of curves, with the associated volumes encoding all possible ψ -class intersection numbers. Although the non-degeneracy of Ω appeared in Kontsevich's original work, the symplectic nature of Ω was not taken advantage of in any particular way.

We develop a recursive formula (an example of *topological recursion*, as explained below) for calculating the symplectic volume of the moduli space of curves. In particular, if $\text{Vol}_{g,n}(L_1, \dots, L_n)$ represents the symplectic volume of $\overline{\mathcal{M}}_{g,n}$, calculated with respect to the symplectic form $\Omega_{\vec{L}}$, then we have

Date: January 23, 2019.

Part of the research for this work was conducted as part of Central Michigan University's REU program in the summer of 2009. J.B., D.C. and K.W. were partially supported by NSF-REU grant #DMS 08-51321.

Theorem 1.1. *The symplectic volumes of moduli spaces of curves obey the recursion relation*

$$\begin{aligned}
(1.1) \quad & L_1 \operatorname{Vol}_{g,n}(L_1, \dots, L_n) \\
&= \sum_{j=2}^n \int_{|L_1-L_j|}^{L_1+L_j} dx \frac{x}{2} (L_1 + L_j - x) \operatorname{Vol}_{g,n-1}(x, L_2, \dots, \hat{L}_j, \dots, L_n) \\
&\quad + \sum_{j=2}^n \int_0^{|L_1-L_j|} dx x f(x, L_1, L_j) \operatorname{Vol}_{g,n-1}(x, L_2, \dots, \hat{L}_j, \dots, L_n) \\
&\quad + \iint_{0 \leq x+y \leq L_1} dx dy \frac{xy}{2} (L_1 - x - y) \operatorname{Vol}_{g-1,n+1}(x, y, L_2, \dots, L_n) \\
&\quad + \sum_{\substack{g_1+g_2=g \\ \mathcal{I} \sqcup \mathcal{J} = \underline{n} \setminus 1}} \iint_{0 \leq x+y \leq L_1} dx dy \frac{xy}{2} (L_1 - x - y) \operatorname{Vol}_{g_1,n_1}(x, L_{\mathcal{I}}) \operatorname{Vol}_{g_2,n_2}(y, L_{\mathcal{J}}),
\end{aligned}$$

subject to the initial conditions

$$(1.2) \quad \operatorname{Vol}_{0,3}(L_1, L_2, L_3) = 1$$

$$(1.3) \quad \operatorname{Vol}_{1,1}(L) = \frac{1}{48} L^2,$$

and $\operatorname{Vol}_{g,n}(L_1, \dots, L_n) = 0$ if $2g - 2 + n < 0$.

The key technique used in the proof involves constructing Hamiltonian torus actions which act locally on moduli space (cf [35] for a related, but different toric symmetry on moduli of curves).

We show that the above recursion has as a simple corollary the DVV formula [6] for ψ -class intersections:

$$\begin{aligned}
(1.4) \quad & \langle \tau_{d_1} \cdots \tau_{d_n} \rangle_g = \sum_{j=2}^n \frac{(2d_1 + 2d_j - 1)!!}{(2d_1 + 1)!!(2d_j - 1)!!} \langle \tau_{d_1+d_j-1} \tau_{d_{\underline{n} \setminus \{1,j\}}} \rangle_g \\
& \quad + \frac{1}{2} \sum_{a+b=d_1-2} \frac{(2a+1)!!(2b+1)!!}{(2d_1+1)!!} \left[\langle \tau_a \tau_b \tau_{d_{\underline{n} \setminus 1}} \rangle_{g-1} \right. \\
& \quad \left. + \sum_{\substack{\text{stable} \\ g_1+g_2=g \\ \mathcal{I} \sqcup \mathcal{J} = \underline{n} \setminus 1}} \langle \tau_a \tau_{d_{\mathcal{I}}} \rangle_{g_1} \langle \tau_b \tau_{d_{\mathcal{J}}} \rangle_{g_2} \right].
\end{aligned}$$

thus providing yet another proof of the Witten-Kontsevich theorem.

In addition, by defining

$$W_{g,n}(z_1, \dots, z_n) = \int_{\mathbb{R}_+^n} e^{-\sum z_i L_i} \operatorname{Vol}_{g,n}(L_1, \dots, L_n) \prod L_i dL_i,$$

and taking the Laplace transform of recursion relation (1.1) we arrive at the equivalent recursion formula

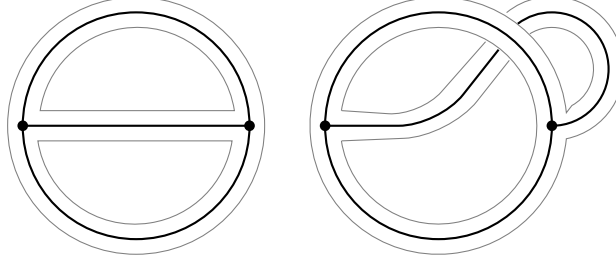
$$\begin{aligned}
 (1.5) \quad W_{g,n}(z_1, \dots, z_n) = & \sum_{j=2}^n -\frac{\partial}{\partial z_j} \left[\frac{z_j}{(z_1 z_j)^2 (z_1^2 - z_j^2)} \left(z_1^2 W_{g,n-1}(z_2, \dots, z_n) \right. \right. \\
 & \left. \left. - z_j^2 W_{g,n-1}(z_1, \dots, \hat{z}_j, \dots, z_n) \right) \right] \\
 & + \frac{1}{2z_1^2} W_{g-1,n+1}(z_1, z_1, \dots, z_n) \\
 & + \frac{1}{2z_1^2} \sum_{\substack{g_1+g_2=g \\ \mathcal{I} \sqcup \mathcal{J} = \underline{n} \setminus 1}} W_{g_1,n_1}(z_1, z_{\mathcal{I}}) W_{g_2,n_2}(z_1, z_{\mathcal{J}}),
 \end{aligned}$$

We prove that (1.5) is an example of the Eynard-Orantin recursion formula [15] for the spectral curve $x = \frac{1}{2}y^2$.

We should emphasize that, apart from recursion equation (1.1), none of the results of the paper are new. For example, there are by now many proofs of the Witten-Kontsevich theorem [21, 32, 20, 26, 19, 35, 30], several of which use techniques similar to what was done in the present work. In addition, it has been shown by Eynard and Orantin [16] that the Airy curve encodes the ψ -class intersection numbers.

Our aim then is not to produce new results in a well-mined field, but rather present a novel point of view which has wider applicability and ramifications. For example, our work makes it geometrically clear *why* it is that the Airy curve encodes intersection numbers - a point of view lacking in the literature. In addition, the techniques developed have a much wider applicability. For example, similar ideas can be used to motivate a generalization of Eynard-Orantin invariants [34] which captures both the generalized Kontsevich matrix model (and in the process intersection numbers of ψ -classes over Witten cycles) and intersection theory for r -spin curves. As well, although the Airy curve is the simplest non-trivial example of the Eynard-Orantin invariants, it is also universal, in the sense that locally all spectral curves look like the Airy curve. Having a good understanding of the local structure of Eynard-Orantin invariants allows one to extrapolate to arbitrary spectral curves by a perturbation type argument [28]. As well, it should be pointed out that the recursion formula proven here played an important role in deriving a new proof [5] of Kontsevich's integration constant $\rho = 2^{5g-5+2n}$, first appearing in [21], relating the symplectic volume of the ribbon graph complex to the Euclidean push-forward measure.

This paper is organized as follows. In Section 2 we survey the definitions and constructions needed in the paper. We define the ribbon graph complex, and the symplectic 2-form Ω originally constructed by Kontsevich. We discuss the relationship to tautological classes on the moduli space of stable curves, and also consider the Eynard-Orantin invariants, focusing on the relevant case of when the spectral curve is \mathbb{P}^1 . Finally, we survey the tools from symplectic geometry which are necessary in the sequel. In Section 3, we construct the local torus symmetries on the ribbon graph complex and show that the associated symplectic quotients are also ribbon graph complexes. In Section 4, we use the local picture to derive recursion equation (1.1), and provide full consideration of the base case volumes (1.2) and

FIGURE 1. Ribbons graphs of type $(0, 3)$ and $(1, 1)$.

(1.3). In Section 5 we prove that our recursion relation is equivalent to the DVV equation (Virasoro constraint) for ψ -class intersections on $\overline{\mathcal{M}}_{g,n}$, while in Section 6 we prove that it is equivalent to the Eynard-Orantin recursion for the spectral curve $x = \frac{1}{2}y^2$.

2. BACKGROUND

2.1. Ribbon graph complexes. A ribbon graph is a graph with a cyclic ordering assigned to the half-edges incident on each vertex. The cyclic ordering allows the edges of the graph to be fattened in a canonical way into ribbons, with the resulting surface having an orientation which induces the cyclic ordering at each vertex. Some examples, along with the associated surfaces, are presented in Figure 1, where the cyclic ordering is implied from the standard counter-clockwise orientation of the plane.

A more precise way of defining ribbon graphs, which better elucidates their automorphisms, comes from using permutation data. Let $\gamma \in S_k$ be a permutation of the set $\underline{k} = \{1, 2, \dots, k\}$. Then the notation (γ) represents the set of disjoint orbits (cycles) or γ , and $|(\gamma)|$ denotes the number of orbits. For example, if $\gamma = (134)(2)(56)$ then $(\gamma) = \{(134), (2), (56)\}$, while $|(\gamma)| = 3$.

Definition 2.1. A ribbon graph is a collection $(\gamma_0, \gamma_1, \gamma_2, b)$ such that

- (1) Each γ_i is a permutation in S_{2k} for some fixed $k > 0$.
- (2) γ_1 is a fixed-point-free involution.
- (3) γ_0 contains no cycles of length 1 or 2.
- (4) $\gamma_2 = \gamma_0^{-1} \circ \gamma_1$, so strictly speaking, is not a necessary part of the definition of the ribbon graph.
- (5) $b : (\gamma_2) \rightarrow \{1, 2, \dots, |(\gamma_2)|\}$ is a bijection.
- (6) The group generated by γ_0 and γ_1 acts transitively on $\underline{2k}$.

The map b is called the boundary labeling of the graph, which will become clear in what follows. We also have the numbers $n = |(\gamma_2)|$, $e = |(\gamma_1)|$ and $v = |(\gamma_0)|$. The *type* of the ribbon graph is the pair (g, n) where

$$g = 1 - \frac{1}{2}(v - e + n).$$

To associate the above definition with an actual graph, we identify (γ_0) with the set of vertices of our graph, (γ_1) with the set of edges and (γ_2) with the set of boundary paths. In particular, we take $|(\gamma_0)|$ vertices and to each vertex we attach a number of half-edges equal to the length of the corresponding cycle in γ_0 . Each

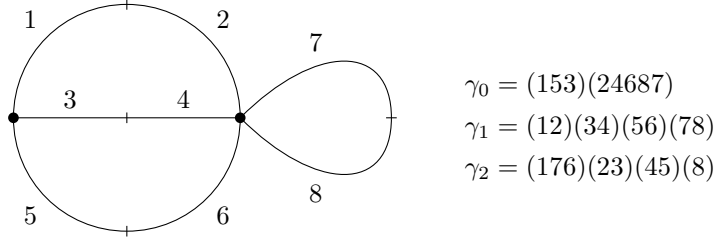


FIGURE 2. Constructing a ribbon graph from half-edge permutations.

vertex can be cyclically ordered by γ_0 . The half-edges are glued to each other by using γ_1 . The construction of the ribbon graph from the permutations is illustrated in Figure 2.

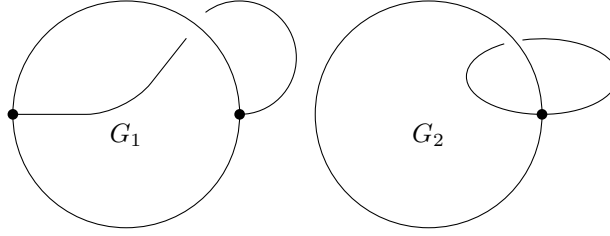
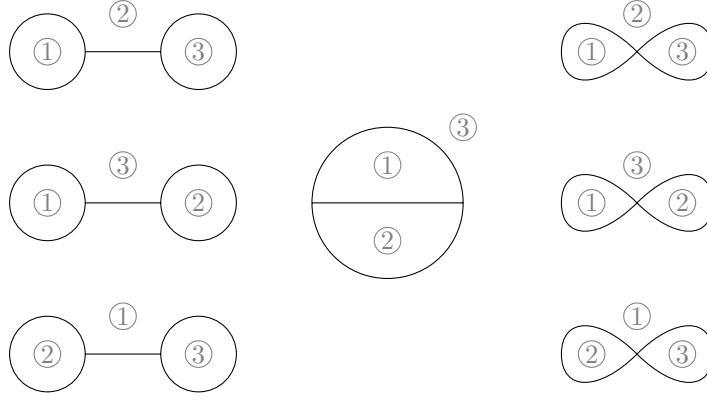
Note that a ribbon graph constructed in this way has its half-edges labeled; however, we do not wish to distinguish ribbon graphs which only differ by their half-edge labelings. This motivates the notion of equivalence of ribbon graphs: Two ribbon graphs (γ_0, γ_1, b) and $(\gamma'_0, \gamma'_1, b')$ are *equivalent* if there is a bijection $\alpha : \underline{2k} \rightarrow \underline{2k}$ such that $\gamma'_i \circ \alpha = \alpha \circ \gamma_i$, and $b = b' \circ \alpha$.

One can, in a canonical way, construct an oriented surface from a ribbon graph by replacing each vertex neighborhood with an oriented disk, then using the edges to attach the disks to each other by ribbons, making sure to preserve the orientation at each vertex. Figure 1 illustrates two ribbon graphs with their associated surfaces. It is straightforward to verify that the surface associated to a given ribbon graph has genus g and n holes, which explains the definition of the type of a graph. Note that condition (6) in the definition forces the graph (and hence surface) to be connected. There are circumstances when a disconnected ribbon graph is allowed, but the changes to the theory are minor and easily worked out.

In what follows, if $j \in \underline{2k}$ then the vertex incident to the half-edge j is denoted $[j]_0$. This can also be thought of as the cycle of γ_0 which contains j . Similarly, the edge containing j is denoted $[j]_1$ while the corresponding boundary component is $[j]_2$. We see that the valence (or degree) of a vertex (number of half-edges incident to it) equals the size of its γ_0 orbit. In particular, condition (3) requires that a ribbon graph has no 1- or 2-valent vertices.

We define $\mathcal{G}_{g,n}$ to be the set of all equivalence classes of ribbon graphs of type (g, n) . Because of the degree restriction on vertices from condition (3), there is an upper bound of $12g - 12 + 6n$ on the number of half-edges of a graph, realized exactly when the graph is *trivalent* – all vertices having degree 3. As a result, there are a finite number of equivalence classes of graphs of a fixed type. Note that, in general, a ribbon graph $G \in \mathcal{G}_{g,n}$ may have automorphisms (self-equivalences) and we let $\text{Aut}(G)$ denote the automorphism group of G . For example, $\mathcal{G}_{1,1}$ consists of two graphs, as pictured in Figure 3, with automorphism groups $\text{Aut}(G_1) = \mathbb{Z}_6$ and $\text{Aut}(G_2) = \mathbb{Z}_4$, while $\mathcal{G}_{0,3}$ consists of seven distinct graphs, presented in Figure 4, all with trivial automorphism groups. Note that the graphs have non-trivial automorphisms which permute the boundaries, which reduce the number of distinct boundary labelings.

A metric on a ribbon graph $G = (\gamma_0, \gamma_1, b)$ is a function $\ell : (\gamma_1) \rightarrow \mathbb{R}_+$, from the set of edges to the positive reals. One can think of a metric as determining the length

FIGURE 3. Set of all ribbon graphs of type $(1, 1)$.FIGURE 4. Set of all ribbon graphs of type $(0, 3)$. Boundary labelings are indicated by the circled numbers.

of each edge of a graph. Note that if $e = |\gamma_1|$ is the number of edges of G , then an element of \mathbb{R}_+^e determines a metric on G . If G has nontrivial automorphisms, they act nontrivially on \mathbb{R}_+^e by permuting the coordinates. Hence, we see that the set of all metrics on a graph is naturally identified with

$$\text{Met}(G) = \mathbb{R}_+^e / \text{Aut}(G),$$

and we define the ribbon graph complex of type (g, n) by

$$\text{RG}_{g,n} = \bigsqcup_{G \in \mathcal{G}_{g,n}} \text{Met}(G).$$

The ribbon graph complex can be given a topology by considering edge collapsing: taking the limit of an edge length to 0, for any non-loop edge, results in a ribbon graph of the same type with the corresponding edge contracted. The resulting set of metric ribbon graphs is glued to the face of the metric set of the larger graph. The resulting topological space has the structure of a connected differentiable orbifold of dimension $6g - 6 + 3n$ [36, 27].

Given a metric ribbon graph, one can assign perimeters to each boundary of the graph by adding together the lengths of all edges which appear on the boundary. Note that, in general, each edge appears on two boundaries (each half edge is part of a boundary), so that it is possible for an edge to contribute twice to a perimeter.

We denote the perimeter map

$$p : \text{RG}_{g,n} \rightarrow \mathbb{R}_+^n.$$

If $L_{\underline{n}}$ denotes the vector $(L_1, \dots, L_n) \in \mathbb{R}_+^n$ then we define

$$\text{RG}_{g,n}(L_{\underline{n}}) = p^{-1}(L_{\underline{n}}).$$

In other words, it is the set of metric ribbon graphs with fixed boundary lengths.

In general, if $\Gamma \in \text{RG}_{g,n}$ is a metric ribbon graph with half edge $i \in \underline{2k}$, we will denote the length of the edge $[i]_1$ by $\ell(\Gamma, i)$. If the graph is clear from the context we will use $\ell_i = \ell(\Gamma, i)$. In addition, the ribbon graph underlying Γ will be denoted by $|\Gamma|$. We can think of the ℓ_i 's as a set of functions (or local coordinates if we choose one i for each edge) defined on $\text{Met}(\Gamma)$.

Let $d(i)$ denote the degree of the vertex $[i]_0$. To each half-edge i we have the vector field

$$\tau_i = \sum_{j=1}^{d(i)-1} (-1)^j \frac{\partial}{\partial \ell_{\gamma_0^j i}}.$$

We also define vector fields assigned to each edge

$$T_i = T_{\gamma_1 i} = \tau_i + \tau_{\gamma_1 i}.$$

In addition to the orbit notation $[i]_j$ described above for vertices, edges and boundaries of a ribbon graph, we also introduce the following edge-length notation: If boundary k contains m_k half-edges we label the lengths of those edges by $\ell_1^{[k]}, \dots, \ell_{m_k}^{[k]}$. Note that the total ordering of the edges must preserve the inherent cyclic ordering of the boundary, but a choice has been made in creating this list (i.e. choosing a distinguished starting edge out of the cyclically ordered boundary edges).

Following Kontsevich [21], we construct n 2-forms on the ribbon graph complex (one for each boundary) by

$$\omega_k = \sum_{i=1}^{m_k-1} \sum_{j=i+1}^{m_k} d\ell_i^{[k]} \wedge d\ell_j^{[k]},$$

then set

$$\Omega = \frac{1}{2} \sum_{k=1}^n \omega_k.$$

Note that Ω is not invariant under changes in the choices of total ordering at each boundary. However, the difference is always an exact form with

$$\Omega - \Omega' = \sum_{i=1}^n a_i dp_i$$

where a_i are constants. Hence $\Omega|_{\text{RG}_{g,n}(L_{\underline{n}})}$ is well-defined. Moreover, Kontsevich [21] proved that it is non-degenerate when restricted to cells corresponding to graphs with no even-valent vertices.

We are led to define

$$\text{Vol}_{g,n}(L_{\underline{n}}) = \int_{\text{RG}_{g,n}(L_{\underline{n}})} e^\Omega = \int_{\text{RG}_{g,n}(L_{\underline{n}})} \frac{1}{d!} \Omega^d,$$

where $d = 3g - 3 + n$.

In general, the dimension of $\text{RG}_{g,n}$ is equal to $6g-6+3n$, which corresponds with the number of edges in a *trivalent* ribbon graph (all vertices have degree 3). Because they play a special role in what follows, we denote $\text{RG}_{g,n}^3$ to be the space of trivalent metric ribbon graphs. Although, strictly speaking, Ω^d is not a volume form, being degenerate on ribbon graphs with even-valent vertices, it is non-degenerate on the top-dimension strata $\text{RG}_{g,n}^3(L_n)$. Since integration over a set of measure 0 does not contribute, the volume is well-defined.

2.2. Intersection theory on $\overline{\mathcal{M}}_{g,n}$. The primary motivation for studying the ribbon graph complex is because of its close connection to the moduli space of curves $\mathcal{M}_{g,n}$. In fact, a result attributed to Mumford, Thurston and Harer [18] states that $\mathcal{M}_{g,n} \times \mathbb{R}_+^n$ is diffeomorphic (in the sense of orbifolds) to $\text{RG}_{g,n}$. This result follows by examining foliations from Strebel differentials on surfaces. A similar result was proven by Bowditch-Epstein [4], and independently by Penner [33] using hyperbolic geometry.

These results were utilized by Kontsevich [21] to great effect in his celebrated proof of the Witten conjecture [37]. By careful analysis of degenerating ribbon graphs, he was able to use the ribbon graph complex in calculating intersection numbers over the Deligne-Mumford compactification of moduli space $\overline{\mathcal{M}}_{g,n}$. To be precise there is a compactification of the ribbon graph complex $\overline{\text{RG}}_{g,n}(L)$ on which the symplectic form Ω extends and a map

$$q : \overline{\mathcal{M}}_{g,n} \rightarrow \overline{\text{RG}}_{g,n}(L)$$

for which $q^*\Omega$ represents the sum tautological classes $\frac{1}{2}(L_1^2\psi_1 + \cdots + L_n^2\psi_n)$.

Hence, one interpretation of the symplectic volume discussed in the previous section is that it encodes all intersections of ψ -classes on $\overline{\mathcal{M}}_{g,n}$. In fact,

$$(2.1) \quad \text{Vol}_{g,n}(L_N) = \sum_{k_1+\cdots+k_n=d} \prod_{j=1}^n \frac{L_j^{2k_j}}{2^{k_j} k_j!} \int_{\overline{\mathcal{M}}_{g,n}} \psi_1^{k_1} \cdots \psi_n^{k_n}.$$

2.3. Eynard-Orantin topological recursion. The topological recursion formula presented in Section 4 fits into the framework developed by Eynard and Orantin [15], which we now proceed to outline.

Consider a plane algebraic curve C specified by a polynomial equation

$$\begin{aligned} C^o &= \{(x, y) \in \mathbb{C}^2 \mid P(x, y) = 0\} \\ C &= \overline{C^o}. \end{aligned}$$

It is convenient to think of x and y as a choice of two meromorphic functions on C . In other words, given a local coordinate $z \in C$ we have

$$\begin{aligned} x &= x(z) \\ y &= y(z). \end{aligned}$$

We require the projection of C onto the x -axis to be *generic*: branch points are isolated and degree at most two (simply ramified).

Note that the theory developed by Eynard and Orantin applies in a wider setting than presented here, but restricting x and y to be rational functions is more than sufficient for our needs, and makes the theory somewhat simpler. In what follows, we make the additional (unnecessary) assumption that $C = \mathbb{P}^1$, with global coordinate z .

To the data of a spectral curve, one can associate an infinite tower of symmetric multilinear meromorphic differentials $\mathcal{W}_{g,n}(z_1, \dots, z_n) = W_{g,n}(z_1, \dots, z_n) dz_1 \otimes \dots \otimes dz_n$ defined on $\text{Sym}^n C$. They are constructed in a recursive manner, by performing residue computations around the branch points of the x -projection.

In particular, the base cases of the recursion are

$$\begin{aligned} \mathcal{W}_{0,1}(z) &= 0 \\ \mathcal{W}_{0,2}(z_1, z_2) &= \frac{dz_1 \otimes dz_2}{(z_1 - z_2)^2}. \end{aligned}$$

$\mathcal{W}_{0,2}$ is the *Cauchy differentiation kernel*, defined by the property that for any function $f : C \rightarrow \mathbb{P}^1$

$$f'(z)dz = \text{Res}_{\zeta \rightarrow z} f(\zeta) \mathcal{W}_{0,2}(\zeta, z).$$

Note that the differentiation kernel is also referred to as the *Bergmann kernel* in the literature [15]. In addition, if C has genus greater than zero, then the \mathcal{A} -cycle integrals of the kernel need to be specified in order to have a unique differential form.

A few additional constructions are necessary to derive the higher-order invariants. The first is a notion of *conjugate point*: Let a_1, \dots, a_k be the branch points of the projection of C onto the x -axis. If $z \in C$ is sufficiently close to a branch point a_i then there is a unique point $\bar{z} \neq z$ with the same x -projection as z (due to the fact that all branch points are simple). Note that unlike complex conjugation, the locally defined involution $z \mapsto \bar{z}$ is holomorphic.

We also make use of the *Eynard kernel*, defined as

$$E_i(z_1, z_2) = \frac{1}{2} \int_{z_1}^{\bar{z}_1} W_{0,2}(\zeta, z_2) d\zeta \frac{dz_2}{(y(z_1) - y(\bar{z}_1)) dx(z_1)},$$

where E_i is defined locally around the branch point a_i (from which the conjugation operation is defined) and the operator on differential forms $\frac{1}{dx(z)}$ means contraction with the vector field

$$\frac{1}{\frac{dx}{dz}} \frac{d}{dz}.$$

Then, the higher order Eynard-Orantin invariants are defined by the recursion formula

$$\begin{aligned} \mathcal{W}_{g,n+1}(z, \underline{z}_n) &= \sum_i \text{Res}_{\zeta \rightarrow a_i} E_i(z, \zeta) \left[\mathcal{W}_{g-1,n+2}(\zeta, \bar{\zeta}, \underline{z}_n) \right. \\ &\quad \left. + \sum_{g_1+g_2=g} \sum_{\mathcal{I} \sqcup \mathcal{J}=\underline{n}} \mathcal{W}_{g_1,|\mathcal{I}|+1}(\zeta, z_{\mathcal{I}}) \mathcal{W}_{g_2,|\mathcal{J}|+1}(\bar{\zeta}, z_{\mathcal{J}}) \right]. \end{aligned}$$

The Eynard-Orantin invariants have appeared in a broad array of seemingly unconnected mathematics. Some highlights include

- (1) The correlation functions for $y = \sin(\sqrt{x})$ are related to (via the Laplace transform) the Weil-Petersson symplectic volumes for moduli spaces of bordered Riemann surfaces [14], and the recursion formula is equivalent to the recursion formula first discovered by Mirzakhani [25, 26] in the context of hyperbolic geometry.
- (2) The recursion for intersection numbers of mixed ψ and κ_1 classes originally discovered by Mulase and Safnuk [29], and then extended to arbitrary κ

- classes by Liu and Xu [22, 23, 24] were put into the framework of topological recursion by Eynard [8].
- (3) Topological recursion can be used to calculate the generating function enumerating partitions with the Plancherel measure [9, 10].
 - (4) Correlation functions for the curve of the mirror dual to a 3-dimensional toric Calabi-Yau manifold are conjectured to generate the Gromov-Witten potential of the manifold. [2, 11, 13].
 - (5) The Lambert curve $x = ye^{-x}$ gives the generating functions for Hurwitz numbers [1, 3, 12], giving a positive resolution to a conjecture raised by Bouchard and Mariño [3].
 - (6) The curve $x = y + 1/y$ was shown by Norbury [31] to compute the number of lattice points in the moduli space of curves. Refer to [5] for a related construction.

The simplest non-trivial example of a spectral curve is the Airy curve

$$\begin{aligned} x &= \frac{1}{2}z^2 \\ y &= z, \end{aligned}$$

which is a rational curve, with global coordinate z . There is a single branch point at $(0, 0)$, with a globally defined involution $z \mapsto -z$.

The Cauchy differentiation kernel for the Riemann sphere is given by

$$\mathcal{W}_{0,2}(z_1, z_2) = \frac{dz_1 \otimes dz_2}{(z_1 - z_2)^2},$$

while the Eynard kernel at the unique branch point is

$$E(z_1, z_2) = \frac{1}{z_1^2 - z_2^2} \frac{dz_2}{2z_1 dz_1}.$$

This yields a recursion formula

$$\begin{aligned} \mathcal{W}_{g,n}(z_1, \dots, z_n) &= \text{Res}_{\zeta \rightarrow 0} \frac{dz_1}{2\zeta(\zeta^2 - z_1^2)d\zeta} \left(\mathcal{W}_{g-1,n+1}(\zeta, -\zeta, z_2, \dots, z_n) \right. \\ (2.2) \quad &\quad \left. + \sum_{\substack{g_1+g_2=g \\ \mathcal{I} \sqcup \mathcal{J} = \underline{n} \setminus \{1\}}} \mathcal{W}_{g_1,n_1}(\zeta, z_{\mathcal{I}}) \mathcal{W}_{g_2,n_2}(-\zeta, z_{\mathcal{J}}) \right) \end{aligned}$$

Applying the Eynard-Orantin recursion to the first few cases gives

$$\begin{aligned} \mathcal{W}_{0,3}(z_1, z_2, z_3) &= \frac{dz_1 \otimes dz_2 \otimes dz_3}{z_1^2 z_2^2 z_3^2} \\ \mathcal{W}_{1,1}(z) &= \frac{dz}{8z^4} \\ \mathcal{W}_{0,4}(z_1, z_2, z_3, z_4) &= 3 \left(\frac{1}{z_1^2} + \frac{1}{z_2^2} + \frac{1}{z_3^2} + \frac{1}{z_4^2} \right) \prod_{i=1}^4 \frac{dz_i}{z_i^2}. \end{aligned}$$

2.4. Symplectic geometry. The goal of the paper is to calculate the symplectic volume of the ribbon graph complex. The technique presented relies on several standard constructions from symplectic geometry which we now review.

The pair (M, ω) is a symplectic manifold if M is a smooth $2n$ -manifold and ω is a closed, non-degenerate 2-form on M . The non-degeneracy condition of ω forces M to be even-dimensional. In general, if (M, ω) is a symplectic manifold then the

top-dimension form $\frac{1}{n}\omega^n$ is everywhere non-degenerate, and therefore is a volume form. In the case that M is compact (or ω^n is integrable) we define

$$\text{Vol}(M, \omega) = \int_M \frac{1}{n!} \omega^n.$$

Note in particular that the symplectic volume depends on the form ω ; however when M is compact the volume is an invariant of the cohomology class of ω .

Suppose that (M, ω) has a k -torus symmetry. In particular, there is a k -parameter group of diffeomorphisms

$$F_{(t_1, \dots, t_k)} : M \rightarrow M$$

satisfying the following conditions:

- (1) $F_{(t_1, \dots, t_k)}$ is a symplectomorphism for all $t = (t_1, \dots, t_k) \in \mathbb{R}^k$, i.e. $F_t^* \omega = \omega$.
- (2) For all $t, t' \in \mathbb{R}^k$, $F_t \circ F_{t'} = F_{t+t'}$.
- (3) There exists $c \in \mathbb{R}_+^k$ with $F_{t+c} = F_t$ for all $t \in \mathbb{R}^k$. The constant c_j is the *period* or circumference of the j -th component of the torus action.

The symplectic torus action encoded by F has k commuting vector fields denoted X_1, \dots, X_k , constructed by taking derivatives of F :

$$X_j(x) = \left. \frac{\partial F_t(x)}{\partial t_j} \right|_{t=0}$$

A symplectic torus action is called *Hamiltonian* if there is, in addition to the above conditions, a map $\mu : M \rightarrow \mathbb{R}^k$ (called the moment map) satisfying the duality condition

$$\iota_{X_j} \omega = d\mu_j.$$

Note that ι_X is the contraction operator, taking the q -form α to the $(q-1)$ -form such that for any collection of vector fields Y_1, \dots, Y_{q-1}

$$\iota_X \alpha(Y_1, \dots, Y_{q-1}) = \alpha(X, Y_1, \dots, Y_{q-1}).$$

A key property of the moment map is that the torus action preserves level sets: $F_t \mu^{-1}(a) \subset \mu^{-1}(a)$ for all $a, t \in \mathbb{R}^k$. In addition, in many situations the quotient of a level set by the torus is still a manifold. We denote the quotient space

$$M_a = \mu^{-1}(a)/\mathbb{T}^k.$$

In fact, it will be a symplectic manifold with a canonical symplectic form ω_a induced from the original symplectic structure. To be precise, let $q : \mu^{-1}(a) \rightarrow M_a$ be the quotient map. If Y_1, Y_2 are two tangent vectors on M_a we choose arbitrary lifts \tilde{Y}_i (i.e. $q_* \tilde{Y}_i = Y_i$), and define

$$\omega_a(Y_1, Y_2) = \omega(\tilde{Y}_1, \tilde{Y}_2).$$

One can check that ω_a is well-defined, closed and non-degenerate.

The above construction is called *symplectic reduction*. The relevance in the present situation is its applications in volume calculations. Let $D \subset \mathbb{R}^k$ be the image of the moment map. By a theorem of Guillemin and Sternberg [17], D is a convex polytope. One can define the Duistermaat-Heckman measure on D by considering the volume form

$$\text{Vol}(M_x) dx_1 \cdots dx_k.$$

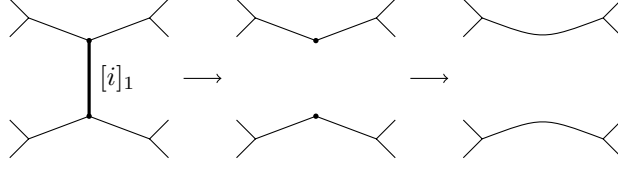


FIGURE 5. Edge removal from a trivalent ribbon graph.

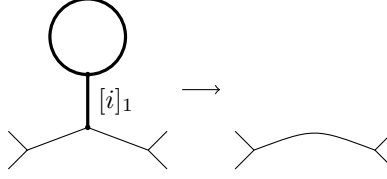


FIGURE 6. Removing a lollipop.

In fact, we have [7]

$$(2.3) \quad \text{Vol}(M) = \int_D \prod c_i \text{Vol}(M_x) dx_1 \cdots dx_k.$$

3. LOCAL STRUCTURE

In this section we construct locally defined Hamiltonian torus actions on the ribbon graph complex. A careful analysis of the domain on which the group action is defined allows for a partition of unity subordinate to the open cover induced by the various domains. As a consequence, one can derive a formula for the volume of the ribbon graph complex by using the symplectic reduction techniques outlined in Section 2.4. The symplectic quotients are themselves ribbon graph complexes, involving graph types of less complexity (where the complexity of a graph of type (g, n) is measured by $2g - 2 + n$). The result is a recursive formula for calculating the symplectic volumes.

Let Γ be a trivalent metric ribbon graph. Given an edge $[i]_1$ we define the metric ribbon graph $\Gamma_{\hat{i}}$ obtained by removing the edge $[i]_1$ from Γ and straightening the resultant 2-valent vertices into contiguous edges, as depicted in Figure 5. The edge lengths of $\Gamma_{\hat{i}}$ are inherited from Γ .

Note that there is an exception to the above operation in case $[i]_1$ adjoins (or is itself) a loop. $\Gamma_{\hat{i}}$ is defined by removing the entire lollipop from Γ , as seen in Figure 6.

If we remember the locations of the deleted vertices, we have two marked points on the boundary of $\Gamma_{\hat{i}}$. Let $m(\Gamma, i)$ denote the number of distinct boundary components on which the markings appear (either 1 or 2). Rotating the marked points can be realized as an m -torus orbit in $\text{RG}_{g,n}$ (if $m = 1$ the marked points must be rotated in sync). We consider the lollipop removal case to also have 1 marked boundary ($m = 1$), since rotation on a simple loop is a trivial action. We call these rotations edge-twist deformations, as one imagines twisting the edge $[i]_1$ around its connections to the remainder of the graph. The infinitesimal generators of these deformations are T_i when it is a circle action and the pair $(\tau_i, \tau_{\gamma_1 i})$ in the case of

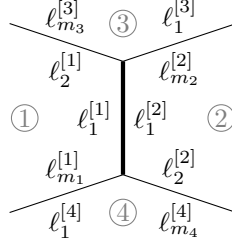


FIGURE 7. Edge labels used to calculate vector field contraction. Note that edge $[i]_1$ is in bold.

a torus action. When edge $[i]_1$ forms a loop, the relevant vector field is $T_{\gamma_0 i} + T_{\gamma_0^2 i}$ (exactly one of the two terms is nonzero).

The set of all ribbon graphs obtained during one complete rotation of edge $[i]_1$ is called the torus orbit of (Γ, i) , and denoted $\mathcal{O}(\Gamma, i)$. For any $\Gamma \in \text{RG}_{g,n}^3(L_{\underline{n}})$ we consider the set

$$\mathcal{U}(\Gamma, i) = \bigcup_{\tilde{\Gamma} \in \text{Met}(|\Gamma|; L_{\underline{n}})} \mathcal{O}(\tilde{\Gamma}, i),$$

where $\text{Met}(|\Gamma|; L_{\underline{n}}) = \text{RG}_{g,n}(L_{\underline{n}}) \cap \text{Met}(|\Gamma|)$. Note that $\mathcal{U}(\Gamma, i) \subset \text{RG}_{g,n}(L_{\underline{n}})$.

If we restrict attention to edges which are adjacent to the first boundary (boundary label 1) we still obtain a cover of the trivalent strata:

$$\text{RG}_{g,n}^3(L_{\underline{n}}) \subset \bigcup_{\Gamma \in \text{RG}_{g,n}^3(L_{\underline{n}})} \bigcup_{i: b(i)=1} \mathcal{U}(\Gamma, i).$$

In addition, each subset $\mathcal{U}(\Gamma, i)$ has a well-defined function $f_{\Gamma, i}(\tilde{\Gamma}) = \ell(\tilde{\Gamma}, i)$.

Lemma 3.1. *The collection of functions $\{\frac{1}{L_1} f_{\Gamma, i}\}$ forms a partition of unity subordinate to the cover $\{\mathcal{U}(\Gamma, i) \mid \Gamma \in \text{RG}_{g,n}^3(L_{\underline{n}}), b_{\Gamma}(i) = 1\}$.*

Proof. This follows from the observation that the sum of edge lengths around the first boundary equals, by definition, L_1 . \square

We note that, by construction, each $\mathcal{U}(\Gamma, i)$ has a globally defined torus action. The dimension of the torus is either 1 or 2, depending on the configuration of the vertices incident to edge $[i]_1$, as discussed earlier.

Lemma 3.2. *The torus action on $\mathcal{U}(\Gamma, i)$ is Hamiltonian, with moment map given by the period(s) of the action.*

Proof. We must calculate the contraction of Ω by the vector fields τ_i and $\tau_{\gamma_1 i}$ in the torus action case and the vector field T_i in the circle action case. Beginning with the case of the circle action, refer to Figure 7 for the notation used in what follows.

Note that the only terms in Ω which contribute are ω_i for $i = 1, 2, 3, 4$. Without loss of generality, we may assume that edge $[i]_1$ corresponds with $\ell_1^{[1]}$ and $\ell_1^{[2]}$, while edge $[\gamma_0 \gamma_1 i]_1$ corresponds with $\ell_1^{[3]}$ and $[\gamma_0 i]_1$ corresponds with $\ell_1^{[4]}$. Under this labeling we have

$$T_i = -\frac{\partial}{\partial \ell_{m_2}^{[2]}} + \frac{\partial}{\partial \ell_2^{[1]}} - \frac{\partial}{\partial \ell_{m_1}^{[1]}} + \frac{\partial}{\partial \ell_2^{[2]}}$$

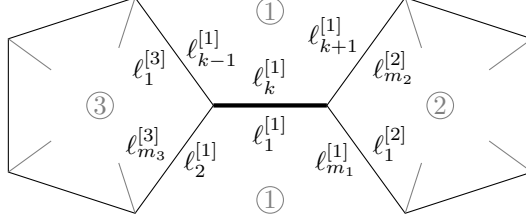


FIGURE 8. Edge labels used to calculate vector field contraction. The edge in bold is $[i]_1$.

$$= -\frac{\partial}{\partial \ell_1^{[3]}} + \frac{\partial}{\partial \ell_{m_3}^{[3]}} - \frac{\partial}{\partial \ell_1^{[4]}} + \frac{\partial}{\partial \ell_{m_4}^{[4]}}.$$

It is straightforward to calculate

$$\begin{aligned} \nu_{T_i} \omega_1 &= -d\ell_1^{[1]} + (d\ell_3^{[1]} + \cdots + d\ell_{m_1}^{[1]}) + (d\ell_1^{[1]} + \cdots + d\ell_{m_1-1}^{[1]}) \\ &= 2dp_1 - 2d\ell_1^{[1]} - d\ell_2^{[1]} - d\ell_{m_1}^{[1]} \\ \nu_{T_i} \omega_2 &= 2dp_2 - 2d\ell_1^{[2]} - d\ell_2^{[2]} - d\ell_{m_2}^{[2]} \\ \nu_{T_i} \omega_3 &= -(d\ell_2^{[3]} + \cdots + d\ell_{m_3}^{[3]}) + (-d\ell_1^{[3]} - \cdots - d\ell_{m_3-1}^{[3]}) \\ &= -2dp_3 + d\ell_1^{[3]} + d\ell_{m_3}^{[3]} \\ \nu_{T_i} \omega_4 &= -2dp_4 + d\ell_1^{[4]} + d\ell_{m_4}^{[4]}. \end{aligned}$$

Note that, although slightly more complicated, nothing fundamentally changes in the above calculation if some of the boundaries happen to agree.

Since $\ell_2^{[1]} = \ell_{m_3}^{[3]}$, $\ell_{m_1}^{[1]} = \ell_1^{[4]}$, $\ell_2^{[2]} = \ell_{m_4}^{[4]}$, $\ell_{m_2}^{[2]} = \ell_1^{[3]}$, and $\ell_1^{[1]} = \ell_i = \ell_1^{[2]}$ (being different labels for the same edges) we have

$$\nu_{T_i} \Omega = d(p_1 + p_2 - 2\ell_i) - dp_3 - dp_4.$$

When restricted to $\text{RG}_{g,n}(L_{\underline{n}})$ we have $dp_k = 0$, and observing that $p_1 + p_2 - 2\ell_i$ is the length of the circle around which edge i rotates completes the first part of the proof.

The torus action case occurs when edge i has the same boundary on either side. Refer to Figure 8 for the notation used in what follows.

When traversing boundary 1, we assume that $\ell_i = \ell_1^{[1]}$, and note that edge i divides the perimeter into two distinct regions (which become the two distinct circles for the torus action). We label $\ell_k^{[1]}$ as the second occurrence of ℓ_i in the perimeter, which makes the two regions labeled by $\ell_2^{[1]}, \dots, \ell_{k-1}^{[1]}$ and $\ell_{k+1}^{[1]}, \dots, \ell_{m_1}^{[1]}$.

The vector fields under this labeling are given by

$$\begin{aligned} \tau_i &= \frac{\partial}{\partial \ell_2^{[1]}} - \frac{\partial}{\partial \ell_{k-1}^{[1]}} \\ &= \frac{\partial}{\partial \ell_{m_3}^{[3]}} - \frac{\partial}{\partial \ell_1^{[3]}} \\ \tau_{\gamma_1 i} &= \frac{\partial}{\partial \ell_{k+1}^{[1]}} - \frac{\partial}{\partial \ell_{m_1}^{[1]}} \end{aligned}$$

$$= \frac{\partial}{\partial \ell_{m_2}^{[2]}} - \frac{\partial}{\partial \ell_1^{[2]}},$$

from which we calculate

$$\begin{aligned} \iota_{\tau_i} \omega_1 &= -d\ell_1^{[1]} + d\ell_3^{[1]} + \cdots + d\ell_{m_1}^{[1]} + d\ell_1^{[1]} + \cdots + d\ell_{k-2}^{[1]} \\ &\quad - (d\ell_k^{[1]} + \cdots + d\ell_{m_1}^{[1]}) \\ &= 2(d\ell_2^{[1]} + \cdots + d\ell_{k-1}^{[1]}) - d\ell_2^{[1]} - d\ell_{k-1}^{[1]} \\ \iota_{\tau_i} \omega_3 &= -(d\ell_2^{[3]} + \cdots + d\ell_{m_3}^{[3]}) - (d\ell_1^{[3]} + \cdots + d\ell_{m_3-1}^{[3]}) \\ &= -2dp_3 + d\ell_1^{[3]} + d\ell_{m_3}^{[3]} \\ \iota_{\tau_{\gamma_1 i}} \omega_1 &= 2(d\ell_{k+1}^{[1]} + \cdots + d\ell_{m_1}^{[1]}) - d\ell_{k+1}^{[1]} - d\ell_{m_1}^{[1]} \\ \iota_{\tau_{\gamma_1 i}} \omega_2 &= -2dp_2 + d\ell_1^{[2]} + d\ell_{m_2}^{[2]}. \end{aligned}$$

By canceling same-edge terms we have

$$\begin{aligned} \iota_{\tau_i} \Omega &= d(\ell_2^{[1]} + \cdots + \ell_{k-1}^{[1]}) - dp_3 \\ \iota_{\tau_{\gamma_1 i}} \Omega &= d(\ell_{k+1}^{[1]} + \cdots + \ell_{m_1}^{[1]}) - dp_2. \end{aligned}$$

Ignoring the inconsequential dp_k terms, we observe that $\ell_2^{[1]} + \cdots + \ell_{k-1}^{[1]}$ is the period of the first circle action, while $\ell_{k+1}^{[1]} + \cdots + \ell_{m_1}^{[1]}$ is the period of the second, thus completing the proof of the lemma. \square

A corollary of the above proof is that Ω restricted to $\text{RG}_{g,n}^3(L)$ is non-degenerate. In fact, the vector fields T_i span the tangent space $T\text{RG}_{g,n}^3(L)$, and the duality relation $\iota_{T_i} \Omega = -2d\ell_i$ completely characterizes Ω .

Note that an alternative description of the moment map is the perimeter map for the newly created boundary (or boundaries) obtained by removing edge $[i]_1$. Hence, the symplectic quotients are identified with subsets of ribbon graph complexes obtained by edge removal. To be precise, the symplectic quotient is a subset of $\text{RG}_{g',n'}$, where (g', n') is the type of the graph Γ_i . In case removing i disconnects Γ into two graphs of type (g_1, n_1) and (g_2, n_2) , then the quotient will be a subset of $\text{RG}_{g_1, n_1} \times \text{RG}_{g_2, n_2}$. Moreover, the perimeters of the newly created graphs are fixed by the original perimeters of Γ and the particular level of the moment map taken for the quotient. A more precise determination of these perimeters and the types of graphs which appear for the quotient is deferred to Section 4.

A consequence of the geometry of the quotients is that they have two independent symplectic structures: $\bar{\Omega}$ coming from symplectic reduction, and Ω induced from the Kontsevich symplectic form on $\text{RG}_{g',n'}$. Although they are defined differently, the two symplectic structures agree:

Lemma 3.3. $\bar{\Omega} = \Omega$.

Proof. Recall that Ω is identified by the duality relation $\Omega(T_i, \cdot) = -2d\ell_i$, while $\bar{\Omega}$ is calculated by lifting vectors to the torus orbit. We denote the quotient map by $q : \mathcal{U}(\Gamma, i) \rightarrow \text{RG}_{g',n'}(L')$, where the exact type and boundaries of the ribbon graph complex in the image is one of the possibilities discussed above. The torus quotient is a local operation, and any edge j not incident to i has $q_* T_j = T_j$, so it remains to find lifts of edges labeled k_1 and k_2 . in Figure 9

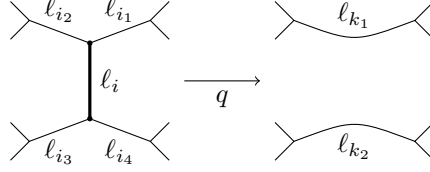


FIGURE 9. Edge notations used to calculate the quotient symplectic form.

However, it is clear that

$$\begin{aligned} q_*(T_{i_1} + T_{i_2}) &= T_{k_1} \\ q_*(T_{i_3} + T_{i_4}) &= T_{k_2}, \end{aligned}$$

while

$$\begin{aligned} \Omega(T_{i_1} + T_{i_2}, \cdot) &= -2(d\ell_{i_1} + d\ell_{i_2}) \\ &= -2d\ell_{k_1} \\ \Omega(T_{i_3} + T_{i_4}, \cdot) &= -2(d\ell_{i_3} + d\ell_{i_4}) \\ &= -2d\ell_{k_2}. \end{aligned}$$

This completes the proof of the lemma. \square

4. RECURSION FORMULA

As constructed in the previous section, we have a partition of unity subordinate to the open cover

$$\{\mathcal{U}(\Gamma, i) \mid \Gamma \in \text{RG}_{g,n}^3(L), \ b(i) = 1\}.$$

Hence we wish to calculate the partition-scaled volume of each $\mathcal{U}(\Gamma, i)$. Rather than calculate each individually, we will group the covers together according to the type and boundary labelings of the edge-deleted graph $\Gamma_{\hat{i}}$. In particular, the different types that arise are:

- (1) Edge i bounds perimeters 1 and j for some $j \neq 1$. In this case, removing edge i is the same as removing a θ -graph with boundary lengths (L_1, L_j, x) , leaving $\Gamma_{\hat{i}} \in \text{RG}_{g,n-1}(x, L_{\underline{n} \setminus \{1,j\}})$ where $|L_1 - L_j| < x < L_1 + L_j$. The length of the edge being removed (value of the partition of unity) is calculated to be

$$\ell_i = \frac{1}{2}(L_1 + L_j - x)$$

- (2) Edge i is part of a lollipop, with boundaries 1 and j on either side (again, $1 \neq j$). We have $\Gamma_{\hat{i}} \in \text{RG}_{g,n-1}(x, L_{\underline{n} \setminus \{1,j\}})$ where $0 \leq x \leq |L_1 - L_j|$. The total length of the lollipop (sum of all edges which contribute to this term) is

$$\begin{cases} L_1 & \text{if } L_1 < L_j \\ L_1 - x & \text{if } L_1 > L_j \end{cases}$$

- (3) Edge i has boundary 1 on both sides, neither vertex has a loop, and removing edge i does not disconnect the graph. Then $\Gamma_i \in \text{RG}_{g-1,n+1}(x, y, L_{\underline{n} \setminus \{1\}})$, where $0 < x + y < L_1$. The length of edge i is calculated to be

$$\ell_i = \frac{1}{2}(L_1 - x - y).$$

- (4) Edge i has boundary 1 on both sides, neither vertex is incident to a loop, and removing edge i disconnects the graph. Then $\Gamma_i \in \text{RG}_{g_1,n_1}(x, L_{\mathcal{I}}) \times \text{RG}_{g_2,n_2}(y, L_{\mathcal{J}})$, where $g_1 + g_2 = g$, $\mathcal{I} \sqcup \mathcal{J} = \underline{n} \setminus \{1\}$, $n_1 = |\mathcal{I}| + 1$ and $n_2 = |\mathcal{J}| + 1$. The newly created boundaries satisfy $0 < x + y < L_1$ and the length of the removed edge is

$$\ell_i = \frac{1}{2}(L_1 - x - y).$$

We note for future reference that if $g_1 = g_2$ and $|\mathcal{I}| = 0 = |\mathcal{J}|$ then there is a symmetry of order 2 obtained by exchanging x and y .

To be clear, there are multiple groupings coming from each of the types listed above. For example, pairs (Γ, i) satisfying type (1) with $j = 2$ are in a different group than pairs satisfying type (1) with $j = 3$. Only type (3) describes a single group.

What makes the integration scheme work is the fact that the symplectic quotients $\mathcal{U}(\Gamma, i)/\mathbb{T}$ of a fixed type form a disjoint cover of the appropriate ribbon graph complex. In other words, the combined reduced volumes of a given type coincides with the volume of the ribbon graph complex of the specified type. This is most easily seen by working backwards. For example, starting with a graph $\Gamma \in \text{RG}_{g,n-1}(x, L_{\underline{n} \setminus \{1,j\}})$, and a point on the boundary of length x , there is a unique way to recover a graph in $\text{RG}_{g,n}(L_{\underline{n}})$: if $x < |L_1 - L_j|$ then one must attach a lollipop to the marked point. If $x > |L_1 - L_j|$ then one must attach a theta graph to the marked point (one of the two vertices of the theta graph must be distinguished in order to perform this operation unambiguously). The other cases are similar.

To calculate the volume of $\text{RG}_{g,n}(L_{\underline{n}})$, we use the partition of unity to write the volume as a sum over torus covers $\mathcal{U}(\Gamma, i)$. We group the covers by type and use the symplectic volume equation (2.3) to calculate the contribution from each grouping. The result is that

$$\begin{aligned}
 (4.1) \quad & L_1 \text{Vol}_{g,n}(L_1, \dots, L_n) \\
 &= \sum_{j=2}^n \int_{|L_1 - L_j|}^{L_1 + L_j} dx \frac{x}{2} (L_1 + L_j - x) \text{Vol}_{g,n-1}(L_{\underline{n} \setminus \{1,j\}}, x) \\
 &+ \sum_{j=2}^n \int_0^{|L_1 - L_j|} dx x f(x, L_1, L_j) \text{Vol}_{g,n-1}(L_{\underline{n} \setminus \{1,j\}}, x) \\
 &+ \iint_{0 \leq x+y \leq L_1} dx dy \frac{xy}{2} (L_1 - x - y) \text{Vol}_{g-1,n+1}(L_{\underline{n} \setminus 1}, x, y) \\
 &+ \sum_{\substack{g_1+g_2=g \\ \mathcal{I} \sqcup \mathcal{J} = \underline{n} \setminus 1}} \iint_{0 \leq x+y \leq L_1} dx dy \frac{xy}{2} (L_1 - x - y) \text{Vol}_{g_1,n_1}(L_{\mathcal{I}}, x) \text{Vol}_{g_2,n_2}(L_{\mathcal{J}}, y),
 \end{aligned}$$

where

$$f(x, y, z) = \begin{cases} y - x & \text{if } y > z \\ y & \text{if } y < z. \end{cases}$$

Note that in the formula above, each integral summand is coming from one of the groupings enumerated above. The integrand consists of the product of periods of the torus action (x or xy) times the appropriate weighting from the partition of unity (length of the edge being removed) times the volume of the symplectic quotient.

The term coming from case (3) has double the edge weighting, due to the fact that the edge appears twice when traversing the boundary. This factor of 2 is compensated by a factor of $\frac{1}{2}$ coming from the fact that when removing the edge from a graph, there is no way to distinguish the two newly created boundaries. Thus, $\text{RG}_{g-1, n+1}(x, y, L_{\underline{n} \setminus 1})$ double counts because the x -length boundary is distinguished from the y -length boundary.

The double-edge contribution in case (4) is compensated for because the sum over $g_1 + g_2 = g$ and $\mathcal{I} \sqcup \mathcal{J} = \underline{n} \setminus 1$ gives a double count over the groupings. The one exception is when $g_1 = g_2$ and $n = 1$. This case only appears once in the sum (if at all), but the factor of $\frac{1}{2}$ is accounted for by the order 2 symmetry of the underlying graph.

The above equation is a *topological recursion* formula for the volumes. In particular, the types of the ribbon graphs appearing on the right hand side are simpler than the type on the left, where the complexity of a graph of type (g, n) can be measured by $2g - 2 + n$. Implicit in the above computation is the fact that $(g, n) \neq (0, 3), (1, 1)$. These can be considered the base cases for the recursion, as all other volume computations can be reduced to knowing $\text{Vol}_{0,3}(L_3)$ and $\text{Vol}_{1,1}(L)$. Luckily, these complexes are simple enough to calculate their volumes by hand, which we now proceed to do.

Volume of $\text{RG}_{0,3}(L_1, L_2, L_3)$. The ribbon graph complex of type $(0, 3)$ has dimension $6g - 6 + 2n = 0$, so we are integrating $\Omega^0 = 1$ over a 0-dimensional space. In other words, $\text{Vol}_{0,3}(L_3)$ is a discrete count of metric ribbon graphs of specified perimeter lengths. The set of all ribbon graphs of type $(0, 3)$ can be found in Figure 4. Note that the automorphism groups are all trivial. Furthermore, once the perimeters are fixed, there is a unique metric ribbon graph which realizes those perimeters.

In particular, if $L_i + L_j > L_k$ for all distinct i, j, k then only the theta graph is possible. The set of perimeter equations

$$\begin{aligned} \ell_1 + \ell_2 &= L_1 \\ \ell_2 + \ell_3 &= L_2 \\ \ell_1 + \ell_3 &= L_3 \end{aligned}$$

has a unique solution with all $\ell_i > 0$. If, for some i, j, k we have $L_i + L_j = L_k$ then the only possible graph is the figure-eight, with the two boundary loops labeled i and j . Finally, if $L_i + L_j < L_k$ for some i, j, k then the graph is a dumbbell, with the loop boundaries labelled by i and j . We conclude that

$$\text{Vol}_{0,3}(L_1, L_2, L_3) = 1.$$

Note that this is the only 0-dimensional ribbon graph complex, and therefore it is the only case where a non-trivalent graph contributes to the volume.

Volume of $\text{RG}_{1,1}(L)$. For graphs of type $(1, 1)$, the dimension of the ribbon graph complex is $6g - 6 + 2n = 2$. Hence we integrate Ω over $\text{RG}_{1,1}(L)$. As illustrated in Figure 3, there is a single graph with the correct number of edges, whose automorphism group is \mathbb{Z}_6 . If the edges are labeled in such a way that when traversing the boundary we encounter (in order) $\ell_1, \ell_2, \ell_3, \ell_1, \ell_2, \ell_3$, then we have

$$\Omega = d\ell_1 \wedge (d\ell_2 + d\ell_3) + d\ell_2 \wedge d\ell_3.$$

If we fix $2(\ell_1 + \ell_2 + \ell_3) = L$ then $d\ell_3 = -d\ell_1 - d\ell_2$ so that

$$\Omega \Big|_{\text{RG}_{1,1}(L)} = d\ell_1 \wedge d\ell_2,$$

and we have

$$\iint_{\ell_1 + \ell_2 \leq \frac{1}{2}L} \Omega = \frac{1}{8}L^2.$$

After dividing by the order of the automorphism group we conclude that

$$\text{Vol}_{1,1}(L) = \frac{1}{48}L^2.$$

5. VIRASORO CONSTRAINTS

The DVV formula [6], or Virasoro constraints, for ψ -class intersections is

$$\begin{aligned} \langle \tau_{d_1} \cdots \tau_{d_n} \rangle_g &= \sum_{j=2}^n \frac{(2d_1 + 2d_j - 1)!!}{(2d_1 + 1)!!(2d_j - 1)!!} \langle \tau_{d_1 + d_j - 1} \tau_{d_{\underline{n} \setminus \{1, j\}}} \rangle_g \\ (5.1) \quad &+ \frac{1}{2} \sum_{a+b=d_1-2} \frac{(2a+1)!!(2b+1)!!}{(2d_1+1)!!} \left[\langle \tau_a \tau_b \tau_{d_{\underline{n} \setminus 1}} \rangle_{g-1} \right. \\ &\quad \left. + \sum_{\substack{\text{stable} \\ g_1+g_2=g \\ \mathcal{I} \sqcup \mathcal{J} = \underline{n} \setminus 1}} \langle \tau_a \tau_{d_{\mathcal{I}}} \rangle_{g_1} \langle \tau_b \tau_{d_{\mathcal{J}}} \rangle_{g_2} \right], \end{aligned}$$

where we are using the notation

$$\langle \tau_{d_1} \cdots \tau_{d_n} \rangle_g = \int_{\overline{\mathcal{M}}_{g,n}} \psi_1^{d_1} \cdots \psi_n^{d_n},$$

and

$$(2k+1)!! = (2k+1)(2k-1) \cdots 1 = \frac{(2k+1)!}{2^k k!}.$$

The stable sum in the last term means we restrict to terms where (g_i, n_i) satisfy $2g_i - 2 + n_i > 0$, where $n_1 = |\mathcal{I}| + 1$ and $n_2 = |\mathcal{J}| + 1$.

The topological recursion formula (4.1) is equivalent to the above DVV relation, if one looks at terms of fixed degree in the L_i 's. To that end, if $P(L_{\underline{n}})$ is a polynomial in L_1^2, \dots, L_n^2 then we denote

$$[d_1 \cdots d_n] P(L_{\underline{n}})$$

to be the coefficient in P of the monomial $L_1^{2d_1} \cdots L_n^{2d_n}$. As seen in (2.1), we have

$$[d_1 \cdots d_n] \text{Vol}_{g,n}(L_{\underline{n}}) = \frac{1}{\prod 2^{d_i} d_i!} \int_{\overline{\mathcal{M}}_{g,n}} \psi_1^{d_1} \cdots \psi_n^{d_n}$$

$$= \frac{1}{\prod 2^{d_i} d_i!} \langle \tau_{d_1} \cdots \tau_{d_n} \rangle_g,$$

where the coefficient is non-zero if and only if $d_1 + \cdots + d_n = d = 3g - 3 + n$.

Note, however, that the topological recursion formula has $L_1 \text{Vol}_{g,n}$ on the left hand side. In fact, it turns out to simplify the calculations if we consider the differentiated topological recursion equation - namely differentiate both sides by L_1 . Then the left hand side gives

$$(5.2) \quad [d_1 \cdots d_n] \frac{\partial}{\partial L_1} L_1 \text{Vol}_{g,n}(L_{\underline{n}}) = \frac{2d_1 + 1}{\prod 2^{d_i} d_i!} \langle \tau_{d_1} \cdots \tau_{d_n} \rangle_g.$$

The differentiated topological recursion formula becomes somewhat simpler:

$$(5.3) \quad \begin{aligned} \frac{\partial}{\partial L_1} L_1 \text{Vol}_{g,n}(L_{\underline{n}}) = & \sum_{j=2}^n \int_0^{L_1+L_j} \frac{x}{2} \text{Vol}_{g,n-1}(x, L_{\underline{n} \setminus \{1,j\}}) dx \\ & + \sum_{j=2}^n \int_0^{|L_1-L_j|} \frac{x}{2} \text{Vol}_{g,n-1}(x, L_{\underline{n} \setminus \{1,j\}}) dx \\ & + \iint_{0 \leq x+y \leq L_1} \frac{xy}{2} \text{Vol}_{g-1,n+1}(x, y, L_{\underline{n} \setminus \{1\}}) dx dy \\ & + \sum_{\substack{g_1+g_2=g \\ \mathcal{I} \sqcup \mathcal{J} = \underline{n} \setminus \{1\}}} \iint_{0 \leq x+y \leq L_1} \frac{xy}{2} \text{Vol}_{g_1,n_1}(x, L_{\mathcal{I}}) \text{Vol}_{g_2,n_2}(y, L_{\mathcal{J}}) dx dy. \end{aligned}$$

To calculate the matching monomial coefficient on the right hand side of the recursion formula, we must explicitly evaluate the above integrals.

For a fixed integer $k \geq 0$ we have

$$(5.4) \quad \begin{aligned} \int_0^{L_1+L_j} \frac{x}{2} x^{2k} dx + \int_0^{|L_1-L_j|} \frac{x}{2} x^{2k} dx &= \frac{1}{2(2k+2)} (L_1 + L_j)^{2k+2} + \frac{1}{2(2k+2)} (L_1 - L_j)^{2k+2} \\ &= \frac{1}{2(2k+2)} \sum_{r=0}^{2k+2} \binom{2k+2}{r} [L_1^r L_j^{2k+2-r} + (-1)^r L_1^r L_j^{2k+2-r}] \\ &= \sum_{s=0}^{k+1} \frac{(2k+1)!}{(2s)!(2k+2-2s)!} L_1^{2s} L_j^{2(k+1-s)}. \end{aligned}$$

By comparing degrees, we see that the coefficient of the $[d_1 \cdots d_n]$ term coming from the above integral is equal to

$$\begin{aligned} & \frac{(2(d_1 + d_j) - 1)!}{(2d_1)!(2d_j)!} [d_1 + d_j - 1 \prod_{i \neq 1,j} d_i] \text{Vol}_{g,n-1}(x, L_{\underline{n} \setminus \{1,j\}}) \\ &= \frac{(2(d_1 + d_j) - 1)!}{(2d_1)!(2d_j)!} \frac{\langle \tau_{d_1+d_j-1} \tau_{\underline{n} \setminus \{1,j\}} \rangle_g}{2^{d_1+d_j-1} 2^{d_{\underline{n} \setminus \{1,j\}}} (d_1 + d_j - 1)! d_{\underline{n} \setminus \{1,j\}}!}. \end{aligned}$$

We also calculate the double integrals by fixing integers $a, b \geq 0$:

$$\iint_{0 \leq x+y \leq L_1} \frac{xy}{2} x^{2a} y^{2b} dx dy = \frac{1}{2} \frac{(2a+1)!(2b+1)!}{(2(a+b+2))!} L_1^{2(a+b+2)}.$$

Hence terms containing $L_1^{2d_1}$ must have $a+b = d_1 - 2$.

Assembling the individual contributions yields

$$\begin{aligned} & \frac{2d_1+1}{\prod 2^{d_i} d_i!} \langle \tau_{d_1} \cdots \tau_{d_n} \rangle_g \\ &= \sum_{j=2}^n \frac{(2(d_1+d_j)-1)!}{(2d_1)!(2d_j)!} \frac{\langle \tau_{d_1+d_j-1} \prod_{i \neq 1,j} \tau_{d_i} \rangle_g}{2^{d_1+d_j-1} (d_1+d_j-1)! \prod_{i \neq 1,j} 2^{d_i} d_i!} \\ &+ \frac{1}{2} \sum_{a+b=d_1-2} \frac{(2a+1)!(2b+1)!}{(2d_1)!} \frac{1}{2^a a! 2^b b!} \frac{1}{\prod_{i \neq 1} 2^{d_i} d_i!} \left[\langle \tau_a \tau_b \prod_{i \neq 1} \tau_{d_i} \rangle_{g-1} \right. \\ &\quad \left. + \sum_{\substack{g_1+g_2=g \\ \mathcal{I} \sqcup \mathcal{J} = \underline{n} \setminus \{1\}}} \langle \tau_a \prod_{i \in \mathcal{I}} \tau_{d_i} \rangle_{g_1} \langle \tau_b \prod_{i \in \mathcal{J}} \tau_{d_i} \rangle_{g_2} \right]. \end{aligned}$$

Canceling matching terms and using the relation

$$(2k-1)!! = \frac{(2k)!}{2^k k!}$$

gives the DVV equation (5.1).

We note that [26, 32, 30] all obtained the same results, in some cases using similar ideas. However, in those situations a scaling limit argument was always needed to access the ψ -class terms. In the present case, the derivation of the DVV is much simpler, due to the fact that no rescaling is necessary.

6. EYNARD-ORANTIN RECURSION

In this section we prove that the topological recursion formula presented above is equivalent to the Eynard-Orantin recursion for the spectral curve $x = \frac{1}{2}y^2$. The main idea is to take the Laplace transform the the recursion formula.

To that end, we define

$$W_{g,n}(z_1, \dots, z_n) = \int \cdots \int e^{-z_{\underline{n}} \cdot L_{\underline{n}}} L_1 \cdots L_n \text{Vol}_{g,n}(L_1, \dots, L_n) dL_1 \cdots dL_n,$$

where $z_{\underline{n}} \cdot L_{\underline{n}} = z_1 L_1 + \cdots z_n L_n$ and the integration is performed over $[0, \infty)^n$. If we take the Laplace transform of $L_2 \cdots L_n$ times the recursion formula then the left hand side becomes $W_{g,n}(z_1, \dots, z_n)$. To evaluate the integrals on the right hand side we swap the order of integration, as explained below.

In general, if $V(x, y)$ denotes a polynomial in x^2 and y^2 and

$$W(z_1, z_2) = \int_0^\infty \int_0^\infty e^{-x z_1 - y z_2} xy V(x, y) dx dy$$

then

$$\begin{aligned}
(6.1) \quad & \int_0^\infty dL_1 e^{-z_1 L_1} \int \int_{0 \leq x+y \leq L_1} dx dy xy (L_1 - x - y) V(x, y) \\
&= \int_0^\infty dx \int_0^\infty dy \int_{x+y}^\infty dL_1 xy \left(-\frac{\partial}{\partial z_1} - (x+y) \right) e^{-z_1 L_1} V(x, y) \\
&= \frac{1}{z_1^2} \int_0^\infty dx \int_0^\infty dy xy V(x, y) e^{-z_1 x - z_1 y} \\
&= \frac{1}{z_1^2} W(z_1, z_1).
\end{aligned}$$

For the term involving boundary j , we define

$$F(x, L_1, L_j) = \begin{cases} L_1 & \text{if } L_1 < L_j, x < L_j - L_1 \\ L_1 - x & \text{if } L_j < L_1, x < L_1 - L_j \\ \frac{1}{2}(L_1 + L_j - x) & \text{if } |L_1 - L_j| < x < L_1 + L_j, \end{cases}$$

then calculate

$$\begin{aligned}
(6.2) \quad & \int_0^\infty dL_j L_j e^{-z_j L_j} \int_0^\infty dL_1 e^{-z_1 L_1} \int_0^{L_1+L_j} dx x F(x, L_1, L_j) V(x) \\
&= -\frac{\partial}{\partial z_j} \left[\frac{1}{z_1^2 z_j (z_1^2 - z_j^2)} (z_1^2 W(z_j) - z_j^2 W(z_1)) \right],
\end{aligned}$$

where we have again adopted the convention that $W(z)$ is the Laplace transform of $xV(x)$, under the assumption that $V(x)$ is a polynomial in x^2 . This equation can be verified by Mathematica, or calculated easily by hand by swapping the order of integration and introducing the change of variables

$$\begin{aligned} u &= L_1 + L_j - x \\ v &= L_j - L_1. \end{aligned}$$

Coming back to the topological recursion formula (4.1), we use (6.2) to calculate the Laplace transform of the first line of the formula, and (6.1) for the remainder of the terms. The result is a recursion formula for $W_{g,n}$:

Lemma 6.1.

$$\begin{aligned}
(6.3) \quad W_{g,n}(z_{\underline{n}}) &= \sum_{j=2}^n -\frac{\partial}{\partial z_j} \left[\frac{z_j}{(z_1 z_j)^2 (z_1^2 - z_j^2)} (z_1^2 W_{g,n-1}(z_{\underline{n} \setminus 1}) - z_j^2 W_{g,n-1}(z_{\underline{n} \setminus j})) \right] \\
&\quad + \frac{1}{2z_1^2} W_{g-1,n+1}(z_1, z_{\underline{n}}) \\
&\quad + \frac{1}{2z_1^2} \sum_{\substack{g_1+g_2=g \\ \mathcal{I} \sqcup \mathcal{J} = \underline{n} \setminus 1}} W_{g_1,n_1}(z_1, z_{\mathcal{I}}) W_{g_2,n_2}(z_1, z_{\mathcal{J}}),
\end{aligned}$$

where $n_1 = |\mathcal{I}| + 1$, $n_2 = |\mathcal{J}| + 1$ and the summation in the last line is taken over all pairs (g_1, \mathcal{I}) , (g_2, \mathcal{J}) subject to the stability condition $2g_i - 2 + n_i > 0$.

The goal is to equate this recursion formula to Eynard-Orantin recursion for the Airy curve $x = \frac{1}{2}y^2$. To do so, we need to explicitly evaluate the residues involved

in (2.2). As a starting point, if we have a function $W(\zeta_1, \zeta_2)$, which we assume to be a polynomial in ζ_1^{-2} and ζ_2^{-2} then we have

$$\begin{aligned} \operatorname{Res}_{\zeta \rightarrow 0} E(\zeta, z_1) W(\zeta, -\zeta) d\zeta \otimes d(-\zeta) &= \operatorname{Res}_{\zeta \rightarrow 0} \frac{-1}{2\zeta} \frac{1}{\zeta^2 - z_1^2} W(\zeta, \zeta) d\zeta \otimes dz_1 \\ &= \frac{1}{2z_1^2} W(z_1, z_1) dz_1. \end{aligned}$$

Recall that the Eynard kernel $E(\zeta, z_1)$ is equal to

$$E(\zeta, z_1) = \frac{1}{2\zeta(\zeta^2 - z_1^2)} \frac{1}{d\zeta} \otimes dz_1.$$

The unstable terms in the Eynard-Orantin recursion have a more complicated residue calculation, due to the diagonal pole in $W_{0,2}$. We have

$$\begin{aligned} \operatorname{Res}_{\zeta \rightarrow 0} E(\zeta, z_1) (W_{0,2}(\zeta, z_j) W(-\zeta) + W_{0,2}(-\zeta, z_j) W(\zeta)) d\zeta \otimes d(-\zeta) \\ = \operatorname{Res}_{\zeta \rightarrow 0} \frac{1}{2\zeta} \frac{-1}{\zeta^2 - z_1^2} \left[\frac{1}{(\zeta - z_j)^2} + \frac{1}{(\zeta + z_j)^2} \right] W(\zeta) d\zeta \otimes dz_1 \\ = \operatorname{Res}_{\zeta \rightarrow 0} \frac{1}{\zeta(z_1^2 - \zeta^2)} \left[-\frac{\partial}{\partial z_j} \frac{z_j}{z_j^2 - \zeta^2} \right] W(\zeta) d\zeta \otimes dz_1, \end{aligned}$$

where we are assuming that $W(\zeta)$ is a polynomial in ζ^{-2} . To finish the calculation, we have the following

Lemma 6.2. *For any integer $k \geq 0$*

$$\operatorname{Res}_{\zeta \rightarrow 0} \frac{1}{\zeta} \frac{1}{z_1^2 - \zeta^2} \frac{1}{z_j^2 - \zeta^2} \zeta^{-2k} d\zeta = \frac{1}{z_1^2 z_j^2 (z_1^2 - z_j^2)} (z_1^2 z_j^{-2k} - z_j^2 z_1^{-2k}).$$

Proof. We expand the left hand side, assuming that ζ is closer to 0 than both z_1 and z_j :

$$\begin{aligned} \operatorname{Res}_{\zeta \rightarrow 0} \frac{1}{z_1^2 - \zeta^2} \frac{1}{z_j^2 - \zeta^2} \zeta^{-2k-1} d\zeta &= \operatorname{Res}_{\zeta \rightarrow 0} \frac{1}{z_1^2 z_j^2} \left(1 + \frac{\zeta^2}{z_1^2} + \dots \right) \left(1 + \frac{\zeta^2}{z_j^2} + \dots \right) \zeta^{-2k-1} d\zeta \\ &= \frac{1}{z_1^2 z_j^2} \sum_{r+s=k} z_1^{-2r} z_j^{-2s} \\ &= \frac{z_1^2 - z_j^2}{z_1^2 z_j^2 (z_1^2 - z_j^2)} \sum_{r=0}^k z_1^{-2r} z_j^{-2(k-r)} \\ &= \frac{1}{z_1^2 z_j^2 (z_1^2 - z_j^2)} (z_1^2 z_j^{-2k} - z_1^{-2k} z_j^2). \end{aligned}$$

□

Putting everything together gives us

Theorem 6.3. *The topological recursion formula (4.1) for the symplectic volume of the ribbon graph complex is equivalent to the Eynard-Orantin recursion for the spectral curve $x = \frac{1}{2}y^2$.*

REFERENCES

- [1] G. Borot, B. Eynard, M. Mulase, and B. Safnuk. A matrix model for simple Hurwitz numbers, and topological recursion, arXiv:0906.1206 [math-ph].
- [2] V. Bouchard, A. Klemm, M. Mariño, and S. Pasquetti. Remodeling the B-model. *Comm. Math. Phys.*, 287(1):117–178, 2009, arXiv:0709.1458 [math.AG].
- [3] V. Bouchard and M. Mariño. Hurwitz numbers, matrix models and enumerative geometry. In *From Hodge theory to integrability and TQFT tt*-geometry*, volume 78 of *Proc. Sympos. Pure Math.*, pages 263–283. Amer. Math. Soc., Providence, RI, 2008, 0709.1458.
- [4] B. H. Bowditch and D. B. A. Epstein. Natural triangulations associated to a surface. *Topology*, 27(1):91–117, 1988.
- [5] K. M. Chapman, M. Mulase, and B. Safnuk. The Kontsevich constants for the volume of the moduli of curves and topological recursion. *ArXiv e-prints*, September 2010, 1009.2055.
- [6] Robbert Dijkgraaf, Herman Verlinde, and Erik Verlinde. Loop equations and Virasoro constraints in nonperturbative two-dimensional quantum gravity. *Nuclear Phys. B*, 348(3):435–456, 1991.
- [7] J. J. Duistermaat and G. J. Heckman. On the variation in the cohomology of the symplectic form of the reduced phase space. *Invent. Math.*, 69(2):259–268, 1982.
- [8] B. Eynard. Recursion between Mumford volumes of moduli spaces, arXiv:0706.4403 [math.AG].
- [9] B. Eynard. All order asymptotic expansion of large partitions. *J. Stat. Mech. Theory Exp.*, (7):P07023, 34, 2008.
- [10] B. Eynard. A matrix model for plane partitions. *J. Stat. Mech. Theory Exp.*, (10):P10011, 72, 2009.
- [11] B. Eynard, A.K. Kashani-Poor, and O. Marchal. A matrix model for the topological string I: Deriving the matrix model, arXiv:1003.1737 [math-ph].
- [12] B. Eynard, M. Mulase, and B. Safnuk. The Laplace transform of the cut-and-join equation and the Bouchard-Marino conjecture on Hurwitz numbers, arXiv:0907.5224 [math.AG].
- [13] B. Eynard and N. Orantin. Geometrical interpretation of the topological recursion, and integrable string theories, arXiv:0911.5096 [math-ph].
- [14] B. Eynard and N. Orantin. Weil-Petersson volume of moduli spaces, Mirzakhani’s recursion and matrix models, arXiv:0705.3600 [math-ph].
- [15] B. Eynard and N. Orantin. Invariants of algebraic curves and topological expansion. *Commun. Number Theory Phys.*, 1(2):347–452, 2007, math-ph/0702045.
- [16] B. Eynard and N. Orantin. Topological recursion in enumerative geometry and random matrices. *J. Phys. A*, 42(29):293001, 117, 2009.
- [17] V. Guillemin and S. Sternberg. Convexity properties of the moment mapping. *Invent. Math.*, 67(3):491–513, 1982.
- [18] John L. Harer. The cohomology of the moduli space of curves. In *Theory of moduli (Montecatini Terme, 1985)*, volume 1337 of *Lecture Notes in Math.*, pages 138–221. Springer, Berlin, 1988.
- [19] M. E. Kazarian and S. K. Lando. An algebro-geometric proof of Witten’s conjecture. *J. Amer. Math. Soc.*, 20(4):1079–1089, 2007.
- [20] Y.-S. Kim and K. Liu. A simple proof of Witten conjecture through localization. *ArXiv Mathematics e-prints*, August 2005, arXiv:math/0508384.
- [21] M. Kontsevich. Intersection theory on the moduli space of curves and the matrix Airy function. *Comm. Math. Phys.*, 147(1):1–23, 1992.
- [22] K. Liu and H. Xu. New properties of the intersection numbers on moduli spaces of curves. *Math. Res. Lett.*, 14(6):1041–1054, 2007, math.AG/0609367.
- [23] K. Liu and H. Xu. New results of intersection numbers on moduli spaces of curves. *Proc. Natl. Acad. Sci. USA*, 104(35):13896–13900 (electronic), 2007, arXiv:0705.3564 [math.AG].
- [24] K. Liu and H. Xu. Recursion formulae of higher Weil-Petersson volumes. *Int. Math. Res. Not. IMRN*, (5):835–859, 2009, arXiv:0708.0565 [math.AG].
- [25] M. Mirzakhani. Simple geodesics and Weil-Petersson volumes of moduli spaces of bordered Riemann surfaces. *Invent. Math.*, 167(1):179–222, 2007.
- [26] M. Mirzakhani. Weil-Petersson volumes and intersection theory on the moduli space of curves. *J. Amer. Math. Soc.*, 20(1):1–23 (electronic), 2007.

- [27] M. Mulase and M. Penkava. Ribbon Graphs, Quadratic Differentials on Riemann Surfaces, and Algebraic Curves Defined over $\overline{\mathbb{Q}}$. *ArXiv Mathematical Physics e-prints*, November 1998, arXiv:math-ph/9811024.
- [28] M. Mulase and B. Safnuk. Combinatorial structures in topological recursion. In preparation.
- [29] M. Mulase and B. Safnuk. Mirzakhani’s recursion relations, Virasoro constraints and the KdV hierarchy. *Indian J. Math.*, 50(1):189–218, 2008, math.QA/0601194.
- [30] M. Mulase and N. Zhang. Polynomial recursion formula for linear Hodge integrals, arXiv:0908.2267 [math.AG].
- [31] P. Norbury. String and dilaton equations for counting lattice points in the moduli space of curves, arXiv:0905.4141 [math.AG].
- [32] A. Okounkov and R. Pandharipande. Gromov-Witten theory, Hurwitz numbers, and matrix models. In *Algebraic geometry—Seattle 2005. Part 1*, volume 80 of *Proc. Sympos. Pure Math.*, pages 325–414. Amer. Math. Soc., Providence, RI, 2009.
- [33] R. C. Penner. The decorated Teichmüller space of punctured surfaces. *Comm. Math. Phys.*, 113(2):299–339, 1987.
- [34] B. Safnuk. Generalizations of topological recursion. In preparation.
- [35] B. Safnuk. Integration on moduli spaces of stable curves through localization. *Differential Geom. Appl.*, 27(2):179–187, 2009, arXiv:0704.2530 [math.DG].
- [36] Daniel D. Sleator, Robert E. Tarjan, and William P. Thurston. Rotation distance, triangulations, and hyperbolic geometry. *J. Amer. Math. Soc.*, 1(3):647–681, 1988.
- [37] E. Witten. Two-dimensional gravity and intersection theory on moduli space. In *Surveys in differential geometry (Cambridge, MA, 1990)*, pages 243–310. Lehigh Univ., Bethlehem, PA, 1991.

BARD COLLEGE

E-mail address: `juliacbennett@gmail.com`

VIRGINIA COMMONWEALTH UNIVERSITY

E-mail address: `cochrandv@vcu.edu`

CENTRAL MICHIGAN UNIVERSITY

E-mail address: `brad.safnuk@cmich.edu`

HARTWICK COLLEGE

E-mail address: `woskoffk@hartwick.edu`